

A novel defined necroptosis-related lncRNAs signature for predicting the prognosis of non-small cell lung cancer

Kui Zhai

Second Affiliated Hospital of Zunyi Medical University

Hao Han

Affiliated Hospital of Zunyi Medical University

Cheng Chen

Affiliated Hospital of Zunyi Medical University

Ming Gong

Affiliated Hospital of Zunyi Medical University

Shixu Fang

Affiliated Hospital of Zunyi Medical University

Kaijun Long

Affiliated Hospital of Zunyi Medical University

Tao Liu

Second Affiliated Hospital of Zunyi Medical University

Xixian Ke

Affiliated Hospital of Zunyi Medical University

Gang Xu (✉ xglhl333@163.com)

Second Affiliated Hospital of Zunyi Medical University

Research Article

Keywords: Necroptosis, lncRNA, non-small cell lung cancer

Posted Date: April 1st, 2022

DOI: <https://doi.org/10.21203/rs.3.rs-1503965/v1>

License:   This work is licensed under a Creative Commons Attribution 4.0 International License.

[Read Full License](#)

Abstract

Background: Faced with the current poor prognosis of non-small cell lung cancer, this topic attempts to find new potential prognostic biomarkers to improve the situation.

Materials and Methods: To form the synthetic matrix, we searched GTEX and The Cancer Genome Atlas for NSCLC transcriptomic data. The necroptosis-related prognostic factor LncRNAs were identified by co-expression analysis and univariate COX regression analysis, and the necroptosis-related LncRNA model was constructed using the least absolute contraction and selection operator (LASSO). Models were then validated using Kaplan-Meier analysis, time-dependent receiver operating characteristics (ROC), univariate COX (uni-COX) regression, multivariate COX (MULTI-COX) regression, nomograms and calibration curves and evaluation. Gene set enrichment analysis (GSEA) was performed in high-risk groups.

Results: We constructed a model containing 4 lncRNAs associated with necroptosis. In the model, we found that the calibration map was in good agreement with prognosis prediction. The 1-, 2-, and 3-year survival rates were 0.663, 0.623, and 0.595, respectively. In conclusion, the results of this project support that necroptosis-related lncRNAs can predict prognosis and help to improve individualized treatment of non-small cell lung cancer.

Conclusion: Necroptosis-related lncRNAs could help to suggest developable therapeutic strategies that would greatly enhance the level of individualized therapy and improve patient outcomes.

Introduction

Lung cancer is one of the malignant tumors that shows the highest global morbidity and mortality (1), and its mortality rate is rising annually. Non-small cell lung cancer (NSCLC) is the most frequent pathological type representing 85% of all lung cancers, with over 4000 new diagnosed cases every year and a 5-year survival rate of approximately 15% (2). Due to the typical concealed characteristic of genesis and development of lung tumors, many NSCLC patients receive their cancer diagnoses at the middle and late stages and miss the opportunity for surgery (3). Statistics from the National Lung Cancer Center in 2016 illustrate that lung cancer is currently the principal cause of morbidity and mortality among malignancies in China. Nevertheless, recent commercialization and clinical expansion of targeted therapies certainly contribute to improving the 5-year survival rate of patients, and targeted therapy has been also adopted as one of the major therapeutic strategies for NSCLC (4). However, some NSCLC patients with contraindications against targeted therapy may develop primary drug resistance or the therapeutic efficacy may be attenuated owing to the presence of coexisting mutations. Although the third-generation EGFR-TKI drugs have shown advantages in the treatment of patients with EGFR-sensitive mutations on the strength of clinical data, primary drug resistance still exists. Furthermore, only patients with EGFR mutation or EGFR T790M mutation benefit from the therapeutics, yet only about 36–48% of advanced NSCLC patients in China are EGFR mutation-positive. As a consequence, not all patients can undergo

targeted therapy(5). Additionally, the drug resistance of targeted therapies is currently high, which forces us to urgently find more new targets, so that more lung cancer patients will benefit from targeted therapies.

Non-coding RNAs (ncRNAs) are non-protein-coding RNAs that can modulate gene expression and protein function. ncRNAs are implicated in all tumors being investigated and can affect all major characteristics related to cancers(6). Additionally, they are also engaged in complicated biological processes, encompassing the development and function of immune cells, immune diseases, etc. Therefore, therapies targeting these naturally occurring ncRNAs against various diseases are a highly promising approach for the treatment of tumors(7).

Long non-coding RNAs (lncRNAs) are a recently identified class of ncRNAs. Human genome encode statistics reveal that the human genome contains more than 16,000 lncRNAs. Although the functions of most lncRNAs have not been substantiated, accumulating evidence suggests the critical cellular functions of lncRNAs(8). A number of lncRNAs control downstream gene expression *via* affecting their transcription, thereby altering the other aspects of biology, such as DNA replication and DNA damage repair responses. Some of which function in diverse gene modulatory mechanisms. Some lncRNAs possess structural and/or regulatory functions and can participate in mRNA splicing, turnover, and translation processes as well as signaling pathways(9). Hence, several cellular functions strongly linked to physiology can be affected by lncRNAs, and alterations in their expression are engaged in the initiation and development of many diseases. The specific expression patterns of these functional lncRNAs exhibit their potential serving as biomarkers for multiple diseases such as human cancers and as attractive therapeutic targets(10).

Given the resistance of most tumors to apoptosis, inducing cell death mechanisms such as necroptosis are strikingly recognized as a promising therapeutic modality against tumors. Necroptosis is a new programmed form of necrotic cells different from apoptosis, and anti-tumor immunity enhancement mediated by CD8⁺ leukocytes upon RIPK1 and RIPK3 activation in the tumor microenvironment (TME) comprises its main mechanism. Meanwhile, necroptosis can accelerate the apoptosis and necrosis of malignant tumor cells by producing immunosuppressive TME through CXCL1 and Mincle, which suggests necroptosis to be a potential immunotherapeutic target against malignant tumors(11–14).

Studies have illustrated that lncRNAs motivate tumor inflammatory response and contribute to immune escape of malignant tumors. The necroptosis-relevant lncRNAs have not been extensively identified, and their functionality in lung cancer has yet to be ascertained. Identification and characteristics of necroptosis-associated lncRNAs can allow us to deeply understand the significance of necroptosis and its related lncRNAs in immunotherapy. Given that the lncRNAs have been highly recognized as novel humoral biomarkers for tumors, we attempted to classify patients according to necroptosis-relevant lncRNAs and determine the relevance of necroptosis-associated lncRNAs and prognosis of NSCLC, to seek more effective therapeutic targets.

Materials And Methods

2.1 Collection of clinical and genetic data of NSCLC patients

The RNA transcriptome dataset (HTSeq-FPKM) and relevant clinical data were downloaded from The Cancer Genome Atlas (TCGA) database to attain the integrated data matrix of lung squamous cell carcinoma, lung adenocarcinoma, and normal lung tissues. To reduce statistical bias in this analysis, NSCLC patients with missing values of overall survival (OS) or short OS (< 30 days) were excluded. A sum of 1037 tissue samples from NSCLC patients and normal 108 lung tissue samples were included.

2.2 Necroptosis-related lncRNA screening

In total, 14,057 lncRNAs were extracted from tissue samples of NSCLC patients and normal lung tissue samples. Combined with previous reports on necroptosis, a map of 67 genes pertaining to necroptosis was finally plotted. The synthesized data matrices were screened employing PERL and LIMMA package of R software(15), followed by correlation analysis between 67 necroptosis-relevant genes and the total lncRNAs in the samples. The lncRNAs conforming to the criterion $\text{corFilter} > 0.6$ and $\text{pvalueFilter} < 0.001$ were deemed as necroptosis-relevant necroptosis. Lastly, 905 lncRNAs conformed to these conditions.

2.3 Construction and validation of risk models

According to the TCGA clinical data of NSCLC patients, the lncRNAs relating to necroptosis were screened utilizing the single-variable Cox proportional hazards regression analysis ($p < 0.05$). Afterwards, LASSO regression with 10-fold cross-validation was implemented for model construction with a p -value of 0.05 and 1,000 running cycles. Receiver operating characteristic (ROC) curves were plotted for 1-, 2-, and 3-year survival of subjects based on the model. The risk score was calculated employing the following formula:

$$\text{Risk score} = \sum_{k=0}^n \text{coef}(\text{LncRNA}^k) * \text{expr}(\text{LncRNA}^k)$$

In this formula, $\text{coef}(\text{LncRNA}^k)$ refers to the coefficient of survival-associated lncRNAs, and $\text{expr}(\text{LncRNA}^k)$ refers to the expression pattern of lncRNAs. With the median risk score serving as the cutoff value, patients were stratified into low-risk and high-risk subgroups, and the relations between the model and clinical factors were assessed by chi-square test to evaluate the prognostic performance of the aforementioned constructed model.

2.4 Independent variable analyses and ROC curves

The predictive potential of different variables for prognosis was estimated with the utility of ROC curves, and single- and multiple-variable COX regression analyses were proceeded for assessing whether risk scores and clinical characteristics were independent variables.

2.5 Nomogram and calibration curve

With the assistance of the RMSR software package, nomograms for 1-, 2-, and 3-year overall survival (OS) and a calibration curve based on the Hosmer-Lemeshow test were generated according to the risk score, age, and tumor (T), node (N), and metastasis (M) stages to illustrate the consistency of the predicted results with real outcomes.

2.6 Gene Set Enrichment Analysis (GSEA)

KEGG (kegg.v7.4.symbols.gmt) and GSEA software (<https://www.gsea-msigdb.org/gsea/login.jsp>) were utilized for enrichment analyses. $p < 0.05$ and $FDR < 0.25$ served as criteria, and JSP was applied to identify remarkably enriched pathways in low- and high-risk populations.

Results

3.1 Identification of lncRNAs pertaining to NSCLC

Using the TCGA matrix, we accessed the data of 108 normal samples and 1037 tumor samples. Based on the expression profiles of 67 necroptosis-related genes and lncRNAs differentially expressed in normal and tumor samples ($|\text{Log}_2\text{FC}| > 1$ and $p < 0.05$) (15, 16), we consequently identified 330 necroptosis-associated lncRNAs (correlation coefficient > 0.4 and $p < 0.001$), consisting of 293 up-regulated lncRNAs and 37 down-regulated lncRNAs (Fig. 1).

3.2 Risk model establishment and verification

The univariable Cox regression analysis offered data revealing the noticeable correlations of 11 necroptosis-associated lncRNAs with OS (all $p < 0.05$). Meanwhile, a heat map was generated. LASSO regression analysis of the aforementioned lncRNAs was implemented to avoid overfitting in the prognostic features. Eventually, 4 lncRNAs (AL590729.1, AC099850.3, AL161757.2, and AC087588.1) were validated. Among these 4 lncRNAs pertaining to necroptosis in NSCLC, the $\text{Log}(\lambda)$ first-order value reflected the probability of a maximum deviation. The Sankey diagram exhibited the positive modulatory correlations of 4 lncRNAs with the necroptosis-associated genes (Fig. 2).

We calculated the risk score with the formula: $\text{risk score} = \text{AL590729.1} \times (-0.9108) + \text{AC099850.3} \times (0.2076) + \text{AL161757.2} \times (-0.9819) + \text{AC087588.1} \times (0.3957)$. We then compared the risk score distribution, patient survival status, survival time, and expression criteria of the above-mentioned lncRNAs between low-risk and high-risk patients in the test set, training set, and all sets. All these results indicated a poor prognosis in the high-risk patients (Fig. 3). Additionally, our analyses of clinicopathological features concerning age, gender, grade, stage, T, N, and M stages illustrated consistent findings (Fig. 4).

3.3 Nomograms for prediction

The hazard ratio (HR) and 95% confidence interval (CI) of univariable COX regression were 1.831 and 1.462–2.247, respectively ($p < 0.001$), and those of the multivariable COX regression were 1.759 and 1.410–2.194, respectively ($p < 0.001$). In the meantime, age (1.0014 and 1.001–1.028; $p = 0.039$), stage (1.438 and 1.275–1.622; $p < 0.001$), T stage (1.200 and 0.996–1.446; $p < 0.056$), N stage (1.421 and

1.229–1.643; $p < 0.001$), and M stage (2.073 and 1.267–3.390; $p = 0.004$) were also independent prognostic parameters. On the strength of 4 independent prognostic variables (risk score, stage, age, and TNM stage), we developed nomograms to predict 1-, 2-, and 3-year OS of NSCLC patients. Also, 1-, 2-, and 3-year calibration curves were utilized to provide evidence demonstrating the consistency of nomograms for prediction with 1-, 2-, and 3-year OS (Fig. 5).

3.4 Risk assessment model

Time-dependent ROC curves were adopted for the sensitivity and specificity assessment of the model for prognosis. Areas under the ROC curves (AUCs) were utilized to illustrate the ROC results, and a larger area was linked to higher evaluation accuracy. The AUCs of 1-, 2-, and 3-year survival were 0.663, 0.623, and 0.595, respectively. Among the clinical characteristics, the AUCs of risk score, age, stage, and T, N, and M stages were 0.663, 0.509, 0.653, 0.628, 0.599, and 0.502, respectively (Fig. 6).

3.5 Pathways enriched in the high-risk population

We applied the GSEA software to identify the KEGG pathways in the high-risk population in all sets to investigate differences in biological functions between risk subgroups. The top 10 pathways enriched in the high-risk population were illustrated to be linked to metastasis, cell cycle, DNA replication, homologous recombination, mismatch repair, nucleic acid excision repair, p53 pathway, cancer pathway, proteasome, and NSCLC pathways (Fig. 7).

Discussion

Although many studies have proposed lncRNAs as molecular markers to forecast the prognosis of NSCLC patients, no study has systematically adopted necroptosis-associated lncRNAs for prognostic prediction in NSCLC patients. This study focused on investigating the utility of necroptosis-relevant lncRNAs as prognostic molecular markers for NSCLC patients. In this study, 67 genes pertaining to necroptosis were collected, and the lncRNAs that could act on these genes were analyzed. Following differential analysis and COX regression analyses, lncRNAs encompassing AL590729.1, AC099850.3, AL161757.2, and AC087588.1 were linked to necroptosis, and the risk models were developed. The models held the promise in serving as independent prognostic indicators of NSCLC and shared significant correlations with the prognosis of NSCLC. Hence, they are promising to be strongly linked to the occurrence, development, and metastasis of NSCLC.

Necroptotic death is a newly unveiled programmed cell death mediated by necroptotic molecules such as ATRX, BRAF, GATA3, and PLK1, with its mechanism similar to apoptosis and morphology similar to necrosis. This form of death possesses paradoxical effects (anti-or pro-tumor).

The study only adopted the public TCGA data for model construction and did not validate the model with our own clinical data due to limited conditions, which is a limitation of our study. In addition, subsequent experiments would be conducted to verify the expression, function, and mechanism of these lncRNAs.

To sum up, our study unraveled the close correlation necroptosis to NSCLC owing to the differential expression patterns of lncRNAs between normal and NSCLC tissues. In addition, models based on 4 necroptosis-associated lncRNAs could serve as independent prognostic molecular markers for NSCLC. This study sheds light on novel lncRNA markers for predicting the prognosis of NSCLC patients and may supply a crucial basis for identifying more genes linked to necroptosis in the future.

Conclusion

Necroptosis-related lncRNAs could help to suggest developable therapeutic strategies that would greatly enhance the level of individualized therapy and improve patient outcomes.

Declarations

Ethics approval and consent to participate: Not applicable.

Consent for publication: Not applicable.

Availability of data and materials: The datasets used analysed during the current study are available from the corresponding author on reasonable request.

Competing interests: The authors declare that they have no competing interests.

Funding: Science and Technology Support Plan of Guizhou Provincial Department of Science and Technology, No.: Qianke He Support [2021] General 081

Authors' contributions:

Project design: Gang Xu and Xixian Ke;

Evaluated the quality of included literature: Cheng Chen, Kaijun Long, Ming Gong Shixu Fang and Tao Liu;

Manuscript writing: Kui Zhai and Hao Han.

Final draft was approved by all the authors.

Acknowledgements: We would like to thank the Science and Technology Support Program of Guizhou Provincial Department of Science and Technology for providing financial support for this project.

References

1. Chen L, Chen F, Li J, Pu Y, Yang C, Wang Y, et al. CAR-T cell therapy for lung cancer: Potential and perspective. *Thorac Cancer*. 2022.

2. Dantas C, Campos Silva S, Tavares Silva D, Santos Silva J, Costa AR, Reis Paulo Calvinho JE. Long Term Follow-up in Surgical Stage I Non-Small Cell Lung Cancer - a Single Center Experience. *Port J Card Thorac Vasc Surg.* 2021;28(2):23–7.
3. Han R, Guan Y, Li M, Xu A, Wu D, Li P, et al. Efficacy and Safety of Nanoadministration in the Treatment of Non-Small-Cell Lung Cancer Is Good to Some Extent: A Systematic Review and Meta-Analysis. *J Oncol.* 2022;2022:9017198.
4. Li N, Liu C, Xiong L, Huang D, Jiang Y. Pedigree analysis of the EGFR p.V1010M germline mutation in a family with a family history of non-small-cell lung cancer. *Ann Transl Med.* 2022;10(3):154.
5. Liu B, Liu H, Ma Y, Ding Q, Zhang M, Liu X, et al. EGFR-mutated stage IV non-small cell lung cancer: What is the role of radiotherapy combined with TKI? *Cancer Med.* 2021.
6. Cao Z, Oyang L, Luo X, Xia L, Hu J, Lin J, et al. The roles of long non-coding RNAs in lung cancer. *J Cancer.* 2022;13(1):174–83.
7. Dai S, Liu T, Liu YY, He Y, Liu T, Xu Z, et al. Long Non-Coding RNAs in Lung Cancer: The Role in Tumor Microenvironment. *Front Cell Dev Biol.* 2021;9:795874.
8. Fan H, Li J, Wang J, Hu Z. Long Non-Coding RNAs (lncRNAs) Tumor-Suppressive Role of lncRNA on Chromosome 8p12 (TSLNC8) Inhibits Tumor Metastasis and Promotes Apoptosis by Regulating Interleukin 6 (IL-6)/Signal Transducer and Activator of Transcription 3 (STAT3)/Hypoxia-Inducible Factor 1-alpha (HIF-1alpha) Signaling Pathway in Non-Small Cell Lung Cancer. *Med Sci Monit.* 2019;25:7624–33.
9. Fang C, Wang L, Gong C, Wu W, Yao C, Zhu S. Long non-coding RNAs: How to regulate the metastasis of non-small-cell lung cancer. *J Cell Mol Med.* 2020;24(6):3282–91.
10. Hu H, Xu H, Lu F, Zhang J, Xu L, Xu S, et al. Exploring the Effect of Differentially Expressed Long Non-coding RNAs Driven by Copy Number Variation on Competing Endogenous RNA Network by Mining Lung Adenocarcinoma Data. *Front Cell Dev Biol.* 2020;8:627436.
11. Tang R, Xu J, Zhang B, Liu J, Liang C, Hua J, et al. Ferroptosis, necroptosis, and pyroptosis in anticancer immunity. *J Hematol Oncol.* 2020;13(1):110.
12. Snyder AG, Hubbard NW, Messmer MN, Kofman SB, Hagan CE, Orozco SL, et al. Intratumoral activation of the necroptotic pathway components RIPK1 and RIPK3 potentiates antitumor immunity. *Sci Immunol.* 2019;4(36).
13. Siempos II, Ma KC, Imamura M, Baron RM, Fredenburgh LE, Huh JW, et al. RIPK3 mediates pathogenesis of experimental ventilator-induced lung injury. *JCI Insight.* 2018;3(9).
14. Yang S, Yu F, Lin M, Sun L, Wei J, Lai C, et al. Single-nucleotide polymorphism rs17548629 in RIPK1 gene may be associated with lung cancer in a young and middle-aged Han Chinese population. *Cancer Cell Int.* 2020;20:143.
15. Meng T, Huang R, Zeng Z, Huang Z, Yin H, Jiao C, et al. Identification of Prognostic and Metastatic Alternative Splicing Signatures in Kidney Renal Clear Cell Carcinoma. *Front Bioeng Biotechnol.* 2019;7:270.

Figures

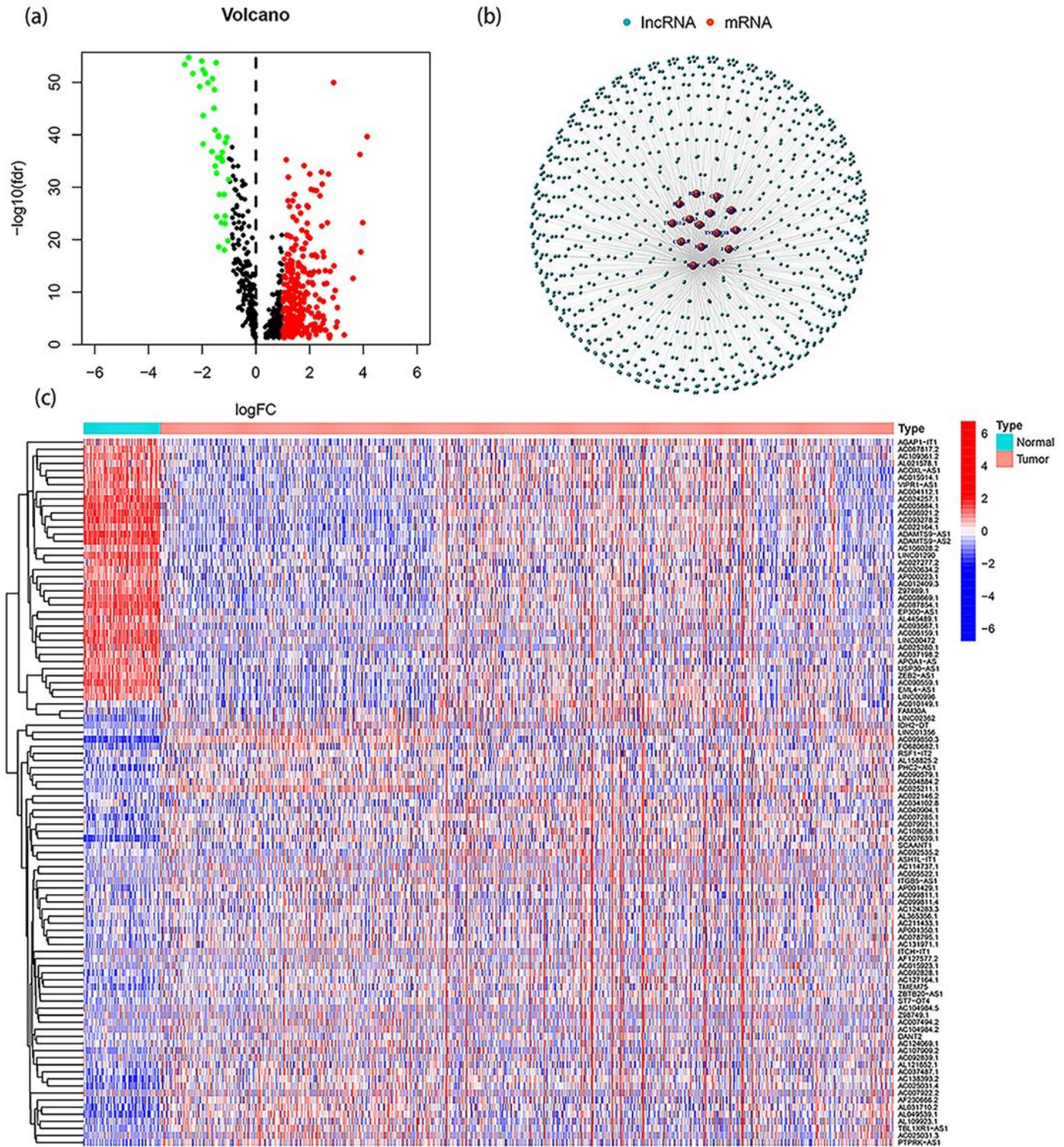


Figure 1

Identification of necroptosis-related lncRNAs in patients with NSCLC.(a)the volcano plot of 330 differentially expressed necroptosis genes.(b)the network between necroptosis genes and lncRNAs (correlation coefficients > 0.6 and p < 0.001).

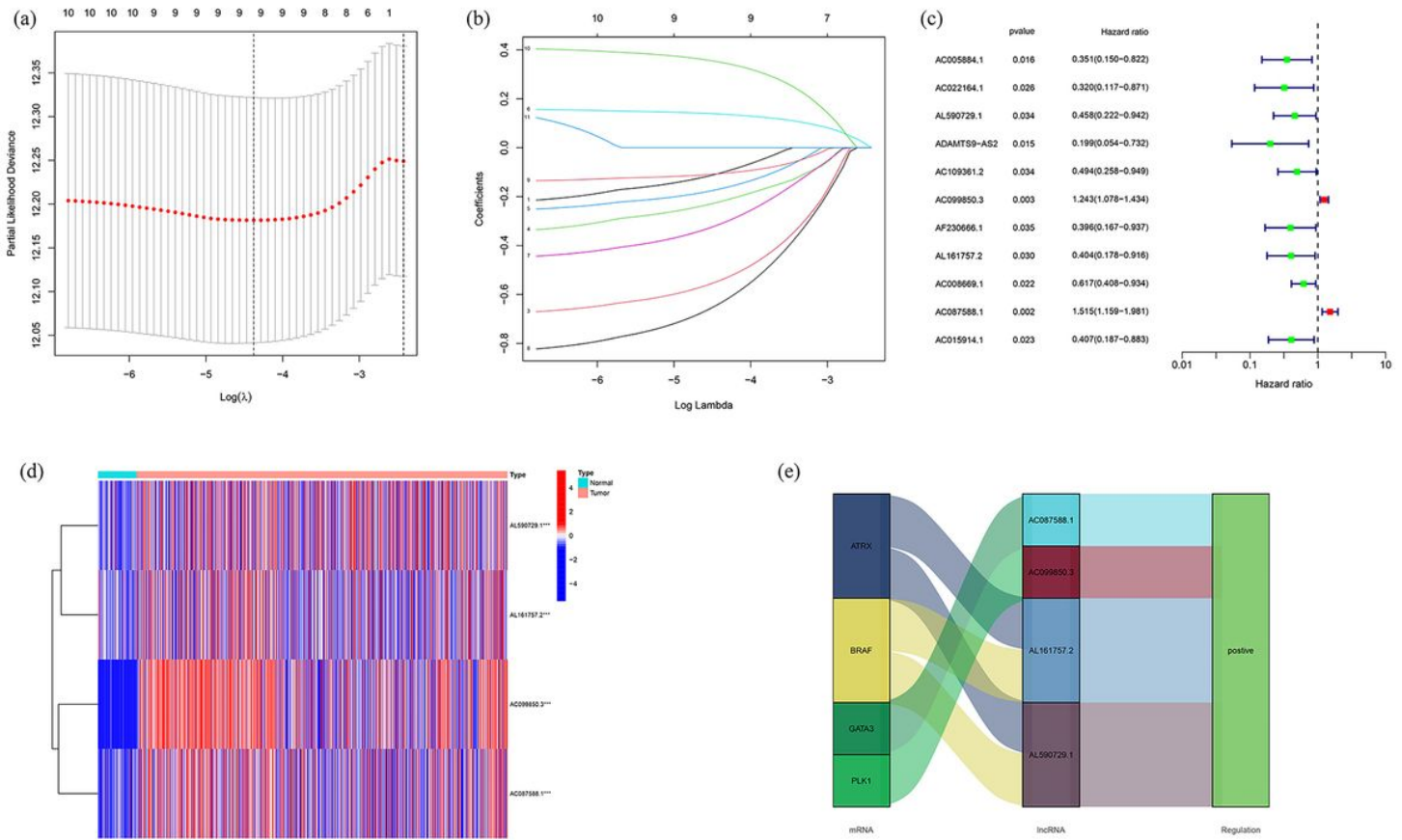


Figure 2

Extraction of necroptosis-related lncRNAs prognostic signature in NSCLC. (a)the LASSO coefficient profile of 11 necroptosis-related lncRNAs. (b)the 10-fold cross-validation for variable selection in the LASSO model. (c) the prognostic lncRNAs extracted by univariate Cox regression analysis. (d)the expression profiles of 4 prognostic lncRNAs. (e)the Sankey diagram of necroptosis genes and related lncRNAs

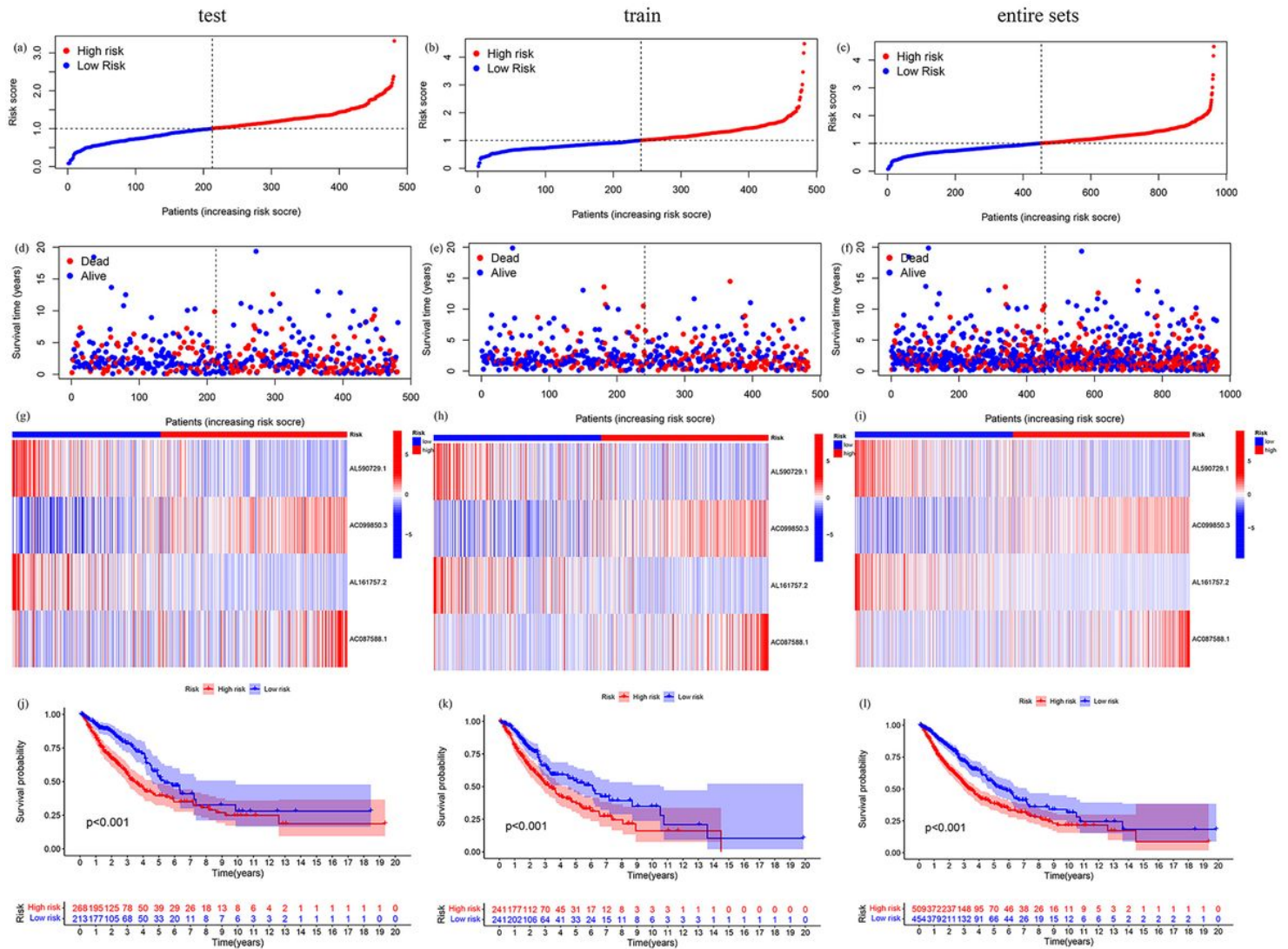


Figure 3

Prognostic value of 16 necroptosis-associated lncRNA models in training, testing, and the whole group. (a-c) Model presentation of necroptosis-related lncRNAs based on training, testing, and full-group risk scores, respectively. (d-f) Survival time and survival status between the low-risk and high-risk groups in the training group, the test group, and the overall group, respectively. (g-i) Heatmaps of 16 lncRNA expression within the training set, test set, and entire set. (j-l) Kaplan-Meier survival curves for OS (probability of survival) of patients in the low-risk group and high-risk group in the train.

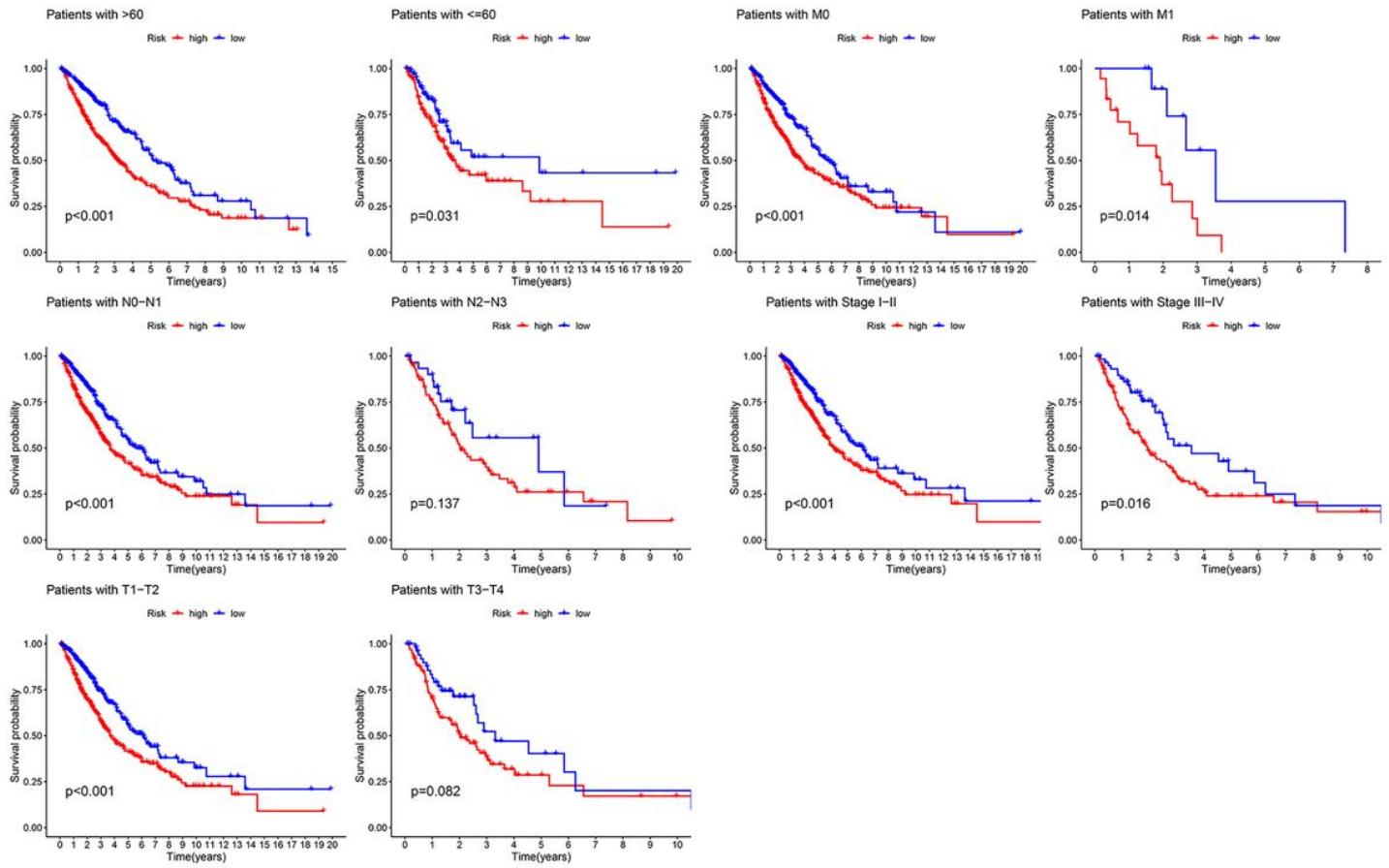


Figure 4

Kaplan-Meier survival curves of OS (probability of survival) prognostic values stratified by age, stage, T, N, or M between low-risk and high-risk groups in the entire set.

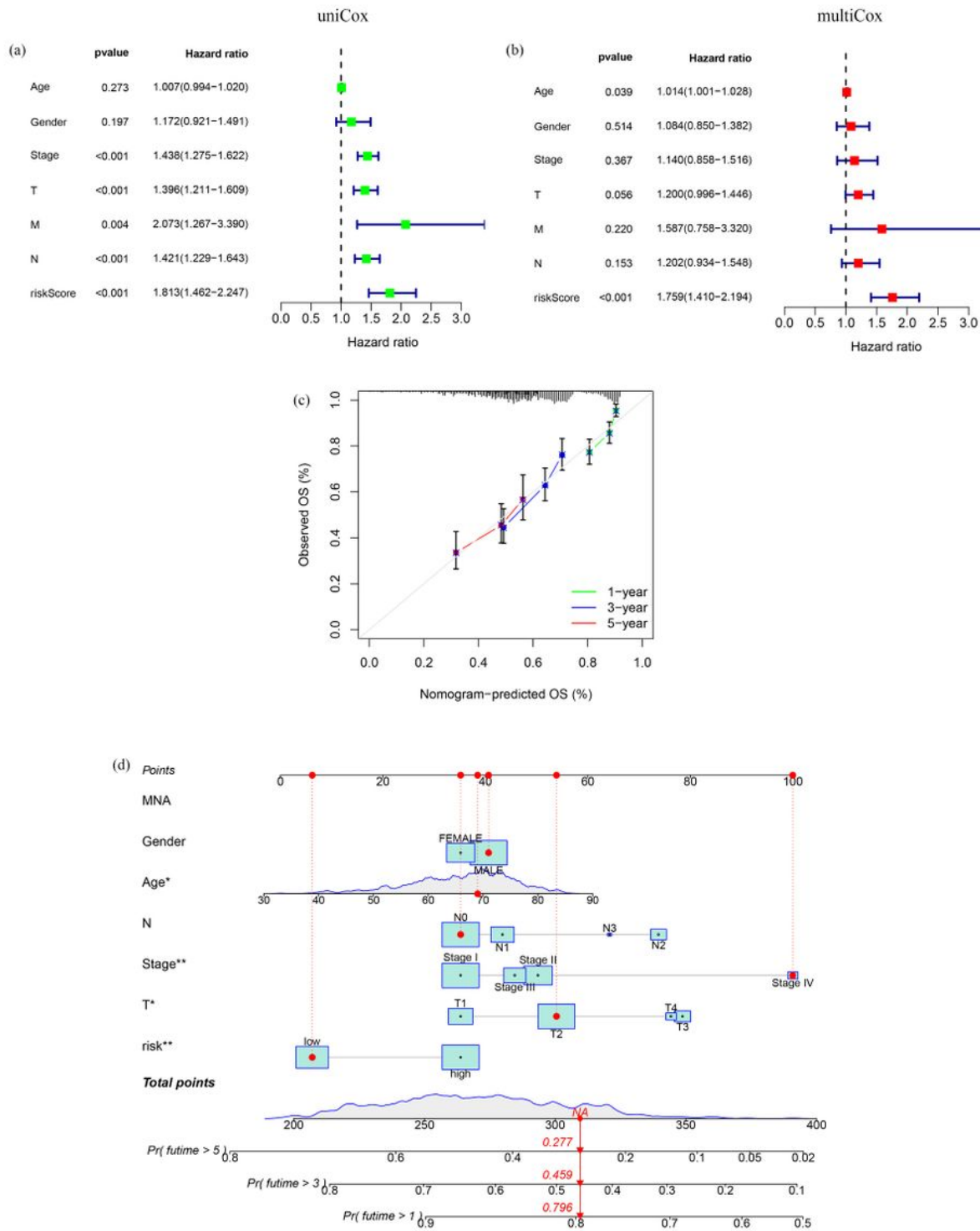


Figure 5

Nomogram and assessment of the risk model. (a, b) Single and multiple Cox analyses of clinical factors and OS risk scores. (c) Calibration curves for 1-, 2-, and 3-year OS. (d) Nomograms of combined risk score, age, and tumor stage predict the probability of 1-, 2-, and 3-year OS.

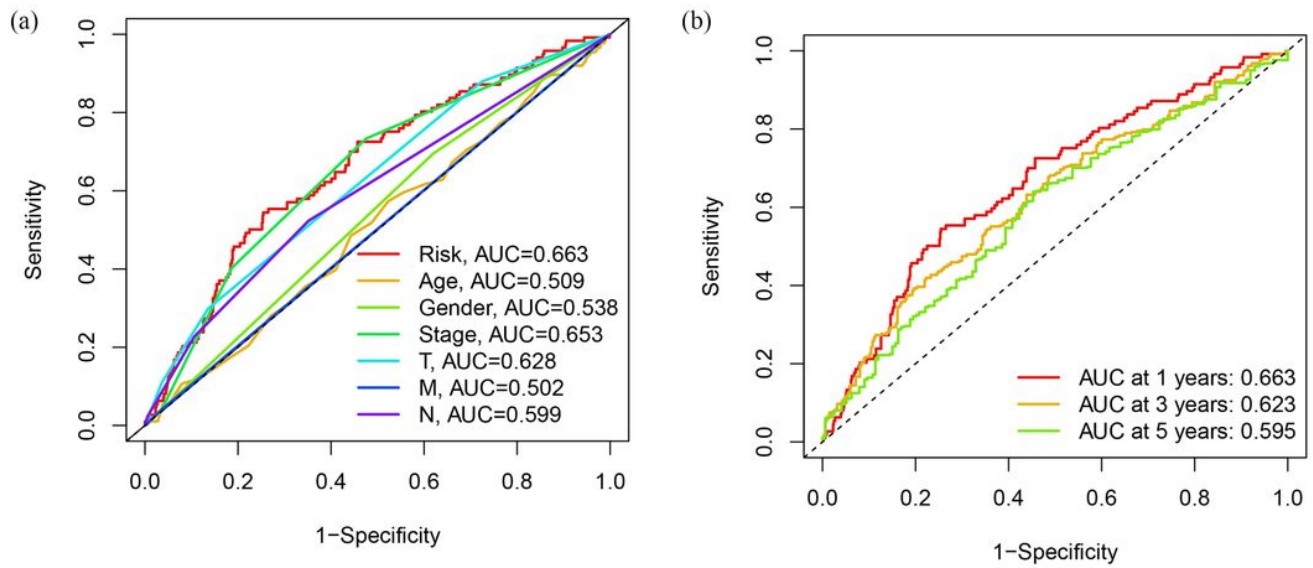


Figure 6

(a) 3-year ROC curves of risk scores, total nomogram scores, and clinical features. (b) 1-year, 2-year and 3-year ROC curves for the training set, test set and full set, respectively.

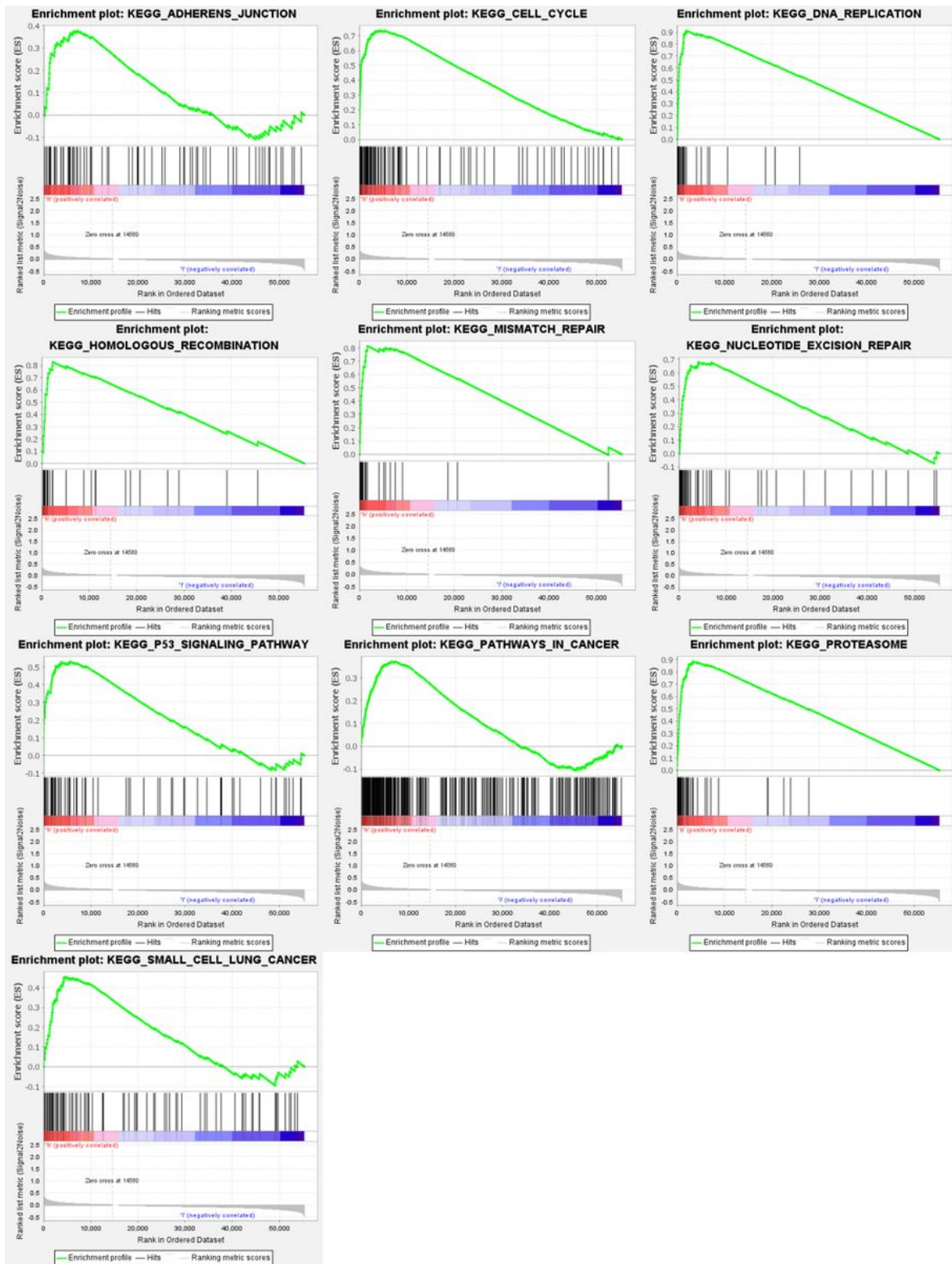


Figure 7

GSEA of cluster.